Biochimica et Biophysica Acta 1783 (2008) 2415–2426

Contents lists available at ScienceDirect

Biochimica et Biophysica Acta

journal homepage: www.elsevier.com/locate/bbamcr

Sun1 forms immobile macromolecular assemblies at the nuclear envelope

Wenshu Lu [a,f], Josef Gotzmann [b,*], Lucia Sironi [c], Verena-Maren Jaeger [a,f], Maria Schneider [a,f], Yvonne Lüke [a], Mathias Uhlén [e], Cristina Al-Khalili Szigyarto [e], Andreas Brachner [b], Jan Ellenberg [c], Roland Foisner [b], Angelika A. Noegel [a,d], Iakowos Karakesisoglou [f,*]

[a] Center for Biochemistry, Medical Faculty, University of Cologne, Joseph-Stelzmann-Strasse 52, 50931 Cologne, Germany
[b] Max F. Perutz Laboratories, Medical University of Vienna, A-1030 Vienna, Austria
[c] Gene Expression and Cell Biology/Biophysics Programmes, European Molecular Biology Laboratory (EMBL), Meyerhofstrasse 1, D-69117 Heidelberg, Germany
[d] Center for Molecular Medicine Cologne, Medical Faculty, University of Cologne, Joseph-Stelzmann-Strasse 52, 50931 Cologne, Germany
[e] The Human Proteome Resource, Department of Biotechnology, Royal Institute of Technology, SE-10691 Stockholm, Sweden
[f] Department of Biological Sciences, The School of Biological and Biomedical Sciences, The University of Durham, DH1 3LE Durham, UK

ARTICLE INFO

Article history:
Received 28 July 2008
Received in revised form 3 September 2008
Accepted 5 September 2008
Available online 19 September 2008

Keywords:
SUN-domain
Sun1
Sun2
Nuclear envelope
Nesprin
KASH-domain
iFRAP

ABSTRACT

SUN-domain proteins form a novel and conserved family of inner nuclear membrane (INM) proteins, which establish physical connections between the nucleoplasm and the cytoskeleton. In the current study, we provide evidence that within the nuclear envelope (NE) Sun1 proteins form highly immobile oligomeric complexes in interphase cells. By performing inverse fluorescence recovery after photobleaching analysis, we demonstrate in vivo that both perinuclear and nucleoplasmic Sun1 segments are essential for maintenance of Sun1 immobility at the NE. Our data in particular underline the self-association properties of the C-terminal coiled-coil Sun1 segment, the ability of which to form dimers and tetramers is demonstrated. Furthermore, the Sun1 tertiary structure involves interchain disulfide bonds that might contribute to higher homo-oligomer formation, although the overall dynamics of the Sun1 C-terminus remains unaffected when the cysteins involved are mutated. While a major Sun1 pool colocalizes with nuclear pore complex proteins, a large fraction of the Sun1 protein assemblies colocalize with immunoreactive foci of Sun2, another SUN-domain paralogue at the NE. We demonstrate that the Sun1 coiled-coil domain permits these heterophilic associations with Sun2. Sun1 therefore provides a non-dynamic platform for the formation of different macromolecular assemblies at the INM. Our data support a model in which SUN-protein-containing multivariate complexes may provide versatile outer nuclear membrane attachment sites for cytoskeletal filaments.

1. Introduction

The nuclear envelope (NE) is a hallmark of eukaryotic cells, functioning as a selective structural barrier separating the cytoplasm from the nucleus. It is composed of a pair of biochemically and functionally distinct membranes, the inner and outer nuclear membranes (INM and ONM, respectively) that are joined together by large macromolecular assemblies the nuclear pore complexes (NPCs) [1]. NPCs form aqueous gated channels spanning the NE regulating the transport of macromolecules between the nucleus and cytoplasm [2,3]. The ONM is continuous with the rough endoplasmic reticulum (ER) and provides attachment sites for cytoplasmic structural elements [4]. In contrast, the INM is composed by a distinct set of membrane proteins, which perform close associations with the underlying nuclear lamina and chromatin [5]. Encompassed by the two NE membranes lies an evenly spaced lumen, the perinuclear space (PNS), which is usually ~20–100 nm in width and continuous with the ER [6].

KASH- and SUN-domain proteins are emerging evolutionarily conserved families of NE-associated molecules [7–9]. From yeast to mammals a conserved mechanism has been established, by which ONM positioned KASH-domain proteins interact with INM positioned SUN-family members in the PNS. These physical "bridges" span both nuclear membranes, thereby providing a structural and possible function-integrating connection between cytoplasmic and nucleoplasmic compartments [7,10–12]. In *C. elegans* and higher eukaryotes, the KASH-domain proteins require SUN-domain proteins for their proper NE localization [10–15]. The majority of KASH-domain proteins appear so far to function as exclusive ONM adaptors mediating interactions with all major cytoskeletal filaments, the centrosome and the microtubule motor protein apparatus [16].

To date, Sad1p in *S. pombe*, Mps3 in *S. cerevisiae*, Dd-Sun1 in *D. discoideum*, UNC-84 and matefin in *C. elegans*, predicted proteins

* Corresponding authors. J. Gotzmann is to be contacted at Max F. Perutz Laboratories, Medical University of Vienna, Vienna, Austria. Tel.: +43 1 4277 61672; fax: +43 1 4277 9616. I. Karakesisoglou, Department of Biological Sciences, The School of Biological and Biomedical Sciences, The University of Durham, DH1 3LE Durham, UK. Tel.: +44 191 3341299; fax: +44 191 3341201.
E-mail addresses: Josef.Gotzmann@meduniwien.ac.at (J. Gotzmann), iakowos.karakesisoglou@durham.ac.uk (I. Karakesisoglou).

0167-4889/$ – see front matter.
doi:10.1016/j.bbamcr.2008.09.001

Q9V996 and Q9VKG2 in *Drosophila*, and human Sun1, Sun2, Sun3, SPAG4 and SPAG4L proteins have been characterized as SUN-domain proteins [8,17–21]. Proteomic approaches, however, indicate their presence in most eukaryotes [18]. Hallmark of the family is the conserved C-terminal SUN-domain (*S*ad1 and *UN*C-84 homology domain) [20]. UNC-84 is independently required for both nuclear migration and nuclear anchorage during *C. elegans* development and might also play a role in lipid metabolism [8]. Sad1p localizes to the spindle pole body and the NE when ectopically overexpressed [22]. Sad1p is essential for viability and required for proper mitotic spindle formation and function [23]. In meiotic cells Rap1p bound telomeres are tethered to Bqt1/Bqt2 complexes, which themselves are connected through Sad1 to the NE, underscoring the essential function of SUN-domain proteins in telomere attachment during meiosis [22]. Interestingly, mouse Sun1 ablation also prevents NE telomere attachment during meiosis and leads to defective gametogenesis [23]. Although controversial results exist, a recent report showed that rat Sun2 is also involved in tethering mammalian meiotic telomeres to the NE [24]. Sun1 is involved in nuclear reassembly after mitosis, regulating chromosome decondensation [25]. Most recently, an association between Sun1, but not Sun2, and the NPCs has been proposed [26].

Besides the SUN-domain, most SUN-domain proteins have at least one predicted transmembrane domain [26] and in addition at least one coiled-coil domain, which in human and mouse Sun1 is proposed to mediate homo and hetero-dimerization with Sun2 [10,11,27]. To date all of them have been identified as exclusive INM components, except SPAG4, which displays an ER-resident localization upon ectopic expression [28]. The N-termini of SUN-proteins all face the nucleoplasm, whereas their C-termini reside in the PNS. Interestingly, the N- and C-termini of mammalian Sun1 can independently localize to the NE [11,26]. However, expression of tagged recombinant Sun1 protein and fragments thereof revealed that Sun1 retention at the NE and association with components of the NPCs require both the nucleoplasmic and luminal domains to a yet unidentified extent [26,28]. The N-termini of UNC-84, SUN-1/Matefin in *C. elegans* and the mammalian Sun1/2 proteins have been shown to associate with the nuclear lamina [20,21,29,30]. However, only UNC-84 requires lamins for its NE localization in nematodes [20].

In this study, we explore in more detail both in vivo and in vitro the Sun1 oligomerization properties and identify the implicated domains. We demonstrate that full-length Sun1 is among the most immobile INM proteins described to date and assign this biological feature to its oligomerization capacity. Truncation of either the nucleoplasmic or luminal Sun1 segments drastically affects its NE dynamics. Our data underline in particular the self-association properties of the C-terminal coiled-coil Sun1 segment, which allows Sun1 tetramerization and permits also heterophilic associations with Sun2. Finally, we provide evidence that SUN-domain proteins assemble into versatile complexes and discuss the biological significance of these macromolecular immobile complexes.

2. Materials and methods

2.1. Cloning strategies

Mouse Sun1 DNA fragments were amplified from IMAGE clone AH48156 by PCR and cloned into pGEMTeasy (Promega) vectors before cloning into GFP, GST or yeast two-hybrid vectors. All GFP-fusion proteins generated carry GFP at their N-terminus. GFP-TM-C (aa 358–913) was cloned into the EcoRI/SalI site of EGFP-C2. GFP-Sun1-FL (aa 1–913), GFP-2TM-N (aa 1–412), GFP-TM-SD1, 2 (aa 358–737), GFP-TM-ΔCC-SUN (aa 358–491, 633–913), GFP-SD1, 2 (aa 432–737) and GFP-SD2 (aa 432–491, 633–737) were cloned into the EcoRI/BamHI site of EGFP-C2. GST-SD1, 2 (aa 432–737) and GST-SD1 (aa 432–632) were cloned into the EcoRI/XhoI site of pGEX4T-1.

Sun1-V5 containing full-length human Sun1 and Sun2-V5-His containing full-length human Sun2 were cloned into pTracer-Vector. hSun1-SD1 (aa 404–493) was cloned into EcoRI/BamHI-digested pGBKT7 and pGADT7. hSun2-CC (aa 400–505) was cloned into the pGADT7 EcoRI/BamHI sites. hSun1 TM-C (aa 240–812) and hSun1 TM-SD1, 2 (aa 240–632) were cloned into the pHA (Roche) or EGFP-C2 HindIII/EcoRI sites.

2.2. Inverse fluorescence recovery after photobleaching experiments (iFRAP)

For live-cell imaging, HeLa cells were transiently transfected with GFP-fusion constructs and examined 48 h after transfection. iFRAPs were performed and normalized as described elsewhere [31]. The fluorescence equilibration between the unbleached and the bleached regions of interest (ROI) in the nucleus was then monitored over a period of up to 10 h. To calculate the loss of fluorescence attributed to the imaging process alone, the sum of pixel intensities was also calculated for the entire cell and used to normalize the fluorescence intensity for each ROI. At least four independent experiments were performed for each construct. We also calculated the relative fluorescence intensity within the bleached areas of the same cells and analyzed these cells by FRAP assays (Fig. S1).

2.3. Antibodies and immunofluorescence microscopy

Western blotting and immunofluorescence (IF) studies were performed as described [32,33]. The following antibodies were used: rabbit polyclonal anti-GST antibody [19], GFP-specific mAb K3-184-2 [34], mouse monoclonal anti-LAP2β (1:250 IF) [35], rat anti-HA antibody (1:250 IF; 1:1000 Western; Sigma), mouse monoclonal anti-V5 antibody (1:5000 Western, 1:500 IF; Invitrogen), mouse monoclonal anti-nuclear pore complex mAb414 (1:5000 IF, Abcam), New rabbit polyclonal antibodies to human Sun1 (Sun1A=HPRK1500010 and Sun1B= HPRK1500015; both 1:400 IF) and Sun2 (HPA001209; 1:500 IF), respectively, were produced within a collaborative project by the Human Proteome Resource [36]. Anti-Sun1 sera 281 were used as described recently [11]. The secondary antibodies used were conjugated with Cy3 (Sigma), FITC (Sigma) and Alexa 568 (Invitrogen). Samples were analyzed by confocal laser-scanning microscopy using either a TCS-SP1 (Leica) or a LSM510-Meta (Zeiss).

2.4. Purification of GST fusion proteins and in vitro binding assays

Purification of GST fusion proteins and GST pull-down experiments were performed as described [37]. The GST free SD1, 2 polypeptides were generated by thrombin digestion of GST-SD1, 2.

2.5. His-tag pull-down assays

GFP-hSun1 and Sun2-V5-His, or GFP and Sun2-V5-His were transiently cotransfected into COS7 cells. The transfected cells were lysed using lysate buffer (50 mM NaH_2PO_4, 150 mM NaCl, 1% NP-40, 0.5% Na-desoxycholate, pH 8.0). Same amount of proteins from each cotransfection were coupled to Ni-NTA agarose beads (Qiagen, Hilden) by incubation for 4 h at 4 °C in 1 ml of lysate buffer. The Ni-NTA agarose beads were washed 5 times with PBS, and 3 times with lysate buffer. The beads were precipitated by centrifugation at 2000 rpm, and proteins bound to the beads were eluted with SDS-sample buffer, resolved by 12% SDS-PAGE and subjected to western blotting analysis.

2.6. Native polyacrylamide gel-electrophoresis (Native-PAGE)

Native gels were prepared similar to SDS-polyacrylamide gels, except that SDS omitted from the gels and buffers employed. Each sample was mixed with 2× native sample buffer (pH 6.8) containing

20% glycerol and 0.01% bromophenol blue in 125 mM Tris–HCl (pH 6.8) and applied onto the native polyacrylamide gel without heating. Native molecular mass markers (Amersham Biosciences) and BSA were used as standards.

2.7. Chemical cross-linking experiments

Cross-linking experiments with the bacterially expressed mouse Sun1 SD1, 2 polypeptides were performed in a buffer containing 20 mM Hepes, pH 8.0, 150 mM NaCl, 5 mM EDTA, and incubated with 0.001%–0.03% glutaraldehyde for 30 min at room temperature. SDS-sample buffer was added to the reactions, and the samples were resolved by 12% SDS-PAGE and stained by Coomassie Blue.

2.8. Yeast two-hybrid assays

The protocols for performing the Yeast two-hybrid analysis are described in detail elsewhere (Yeast Protocols Handbook PT3024-1; Clontech).

2.9. Site-directed mutagenesis

Construction of the point mutant (C526A) in human Sun1 TMC-HA and TMSD1, 2-HA was done with the QuikChange XL Site-Directed Mutagenesis Kit (Stratagene, La Jolla, CA) as described in the manual using the following primers: tmcDelta526sense: 5′-GCGACACGTGAA-GACCGGCGCCGAGACAGTGGATGCCGTAC-3′ and tmcDelta526anti-sense: 5′-GTACGGCATCCACTGTCTCGGCGCCGGTCTTCACGTGTCGC-3′. The mutations were verified by DNA sequencing.

2.10. Immunohistochemistry

Formalin-fixed and paraffin-embedded tissue microarray slides from human tissue were, after deparaffinization, subjected to antigen retrieval by heat induction in Tris-EDTA, pH 9 at 125 °C for 4 min in a pressure boiler. The sections were incubated with the new antisera directed against human Sun-proteins (Sun1A, 1:250; Sun1B, 1:250 and Sun2, 1:150), washed and incubated with a peroxidase-coupled anti-rabbit antibody (Dako). Immunoreactivity as a brownish-black colour was assayed after final incubation with DAB chromagen. All tissue sections were counterstained with hematoxylin. These antibodies are now available at http://www.atlasantibodies.com/home.

3. Results

3.1. Sun1 is a highly immobile NE-associated protein, requiring both N- and C-termini for sustained immobility

To investigate more precisely the Sun1 kinetic properties at the NE, we performed inverse fluorescence recovery after photobleaching experiments (iFRAPs) in interphase cells using GFP-tagged Sun1 full-length (GFP-Sun1-FL) and various N- and C-terminal polypeptides containing different functional domains, respectively (Fig. 1A). iFRAPs are more suitable to analyze binding interactions than classical fluorescence recovery after photobleaching assays (FRAP) because the free pool of the tagged protein is bleached away, allowing precise measurement of the fluorescence changes reflecting the pool of NE-tethered molecules only. The NE topologies of the Sun1 GFP-fusions were verified by implementing membrane-selective permeabilization assays ([38]; Fig. 1B–F). All used Sun1 GFP-fusion proteins displayed an expected INM localization, although varying in prominence. For the iFRAP experiments the whole cell except ~1/3 of the NE region was bleached. GFP-Sun1-FL fluorescence in the unbleached area dropped very slowly and had not completely equilibrated within the bleached area after 10 h (Fig. 2A), indicating that a large proportion of Sun1 at the nuclear membrane is highly immobile within the examined time frame. GFP-N-2TM and GFP-TM-C also display enriched localization at the NE. In many cases we also observed, however, an accumulation of the fusion proteins in the ER or perinuclear aggregates as shown in the pre-bleach images of Fig. 2B and C (arrows). GFP-N-2TM equilibrated after about 35 min and GFP-TM-C after about 29 min (Fig. 2B and C). Thus, both constructs display similar moderately dynamic binding and a significantly reduced immobilization at the NE, when compared to GFP-Sun1-FL. These dynamics data could also be corroborated by performing an alternative bleaching tool, namely fluorescence recovery after photobleaching (FRAP) assays (Fig. S1). Thus, these results suggest that both Sun1 N- and C- termini are required to keep Sun1 immobile and also underscore the initial finding that these domains independently from each other maintain Sun1's stable localization at the NE [11].

Although the Sun1 N-terminus interacts with lamin A, the presence of lamin A/C is not required for Sun1 NE localization [11,28,29]. Therefore, Sun1 was proposed to bind to additional nuclear factors. In fact chromatin immunoprecipitation assays (ChIP) indicate that Sun1 is able to interact with chromatin (data not shown), which has been also reported by Chi et al. [25].

3.2. The SD1-domain is a crucial determinant for reduced Sun1 dynamics at the INM

GFP-TM-SD1, 2 and GFP-TM-ΔCC-SUN appear equally distributed between the NE and the peripheral ER, as indicated in the pre-bleach images (Fig. 2D and E). GFP-TM-SD1, 2 equilibrated after ~26 min (Fig. 2D plot), very similar to GFP-TM-C and GFP-N-2TM. By contrast, for GFP-TM-ΔCC-SUN a major fraction of the fluorescence signal dropped rapidly within the first 2 min, equilibrating within ~8–10 min (Fig. 2E), thus displaying more rapid kinetics than GFP-TM-C and GFP-TM-SD1, 2 indicating transient NE binding. The latter construct containing the SD1-domain (the predicted coiled-coil region; aa 432–632) and lacking the SUN-domain appears even more stable than GFP-TM-ΔCC-SUN, which contains the SUN-domain but lacks the SD1-domain. These in vivo data provide evidence that the SUN-domain confers a kinetically more dynamic attachment to the NE compared to the N-terminus and the lumenal SD1-domain.

We next examined the biochemical fractionation properties of GFP-TM-C and GFP-TM-ΔCC-SUN-proteins. Nuclear fractions of COS7 cells overexpressing equal amounts of these GFP-fusions were extracted with buffers containing urea, non-ionic detergents, or a combination of the latter with high-salt concentrations. The distribution of GFP-fusion proteins in soluble (S) and insoluble (I) fractions was analyzed by immunoblot analysis (Fig. 3A). The well-characterized INM protein LAP2β served as a control. As shown in Fig. 3A, GFP-TM-C was resistant to Triton X-100 extraction and slightly soluble in Triton X-100/high-salt buffer. On the other hand, GFP-TM-ΔCC-SUN was partially soluble upon Triton X-100 treatment and was efficiently extracted by Triton X-100/high-salt-containing buffer. Moreover, none of the two GFP-fusion proteins was extractable with 7 M urea, indicating therefore the anticipated association within nuclear membranes. Collectively, our data unravel the Sun1 SD1 segment as an important stabilizing and potential interaction domain, which has a major impact on Sun1 dynamics.

3.3. Mammalian Sun1 oligomerizes via its SD1-domain

To further investigate biochemically the Sun1 C-terminal domain properties in vitro, we recombinantly purified the SD1, 2-segments and performed Native-PAGE and cross-linking assays. SDS-PAGE analysis of the purified SD1, 2 fragments demonstrated that under reduced conditions the protein migrates as a monomer (32 kDa) (Fig. 3B, left panel). In contrast, Native-PAGE analysis (Fig. 3B, right panel) demonstrated that SD1, 2 proteins migrate preferentially as dimers

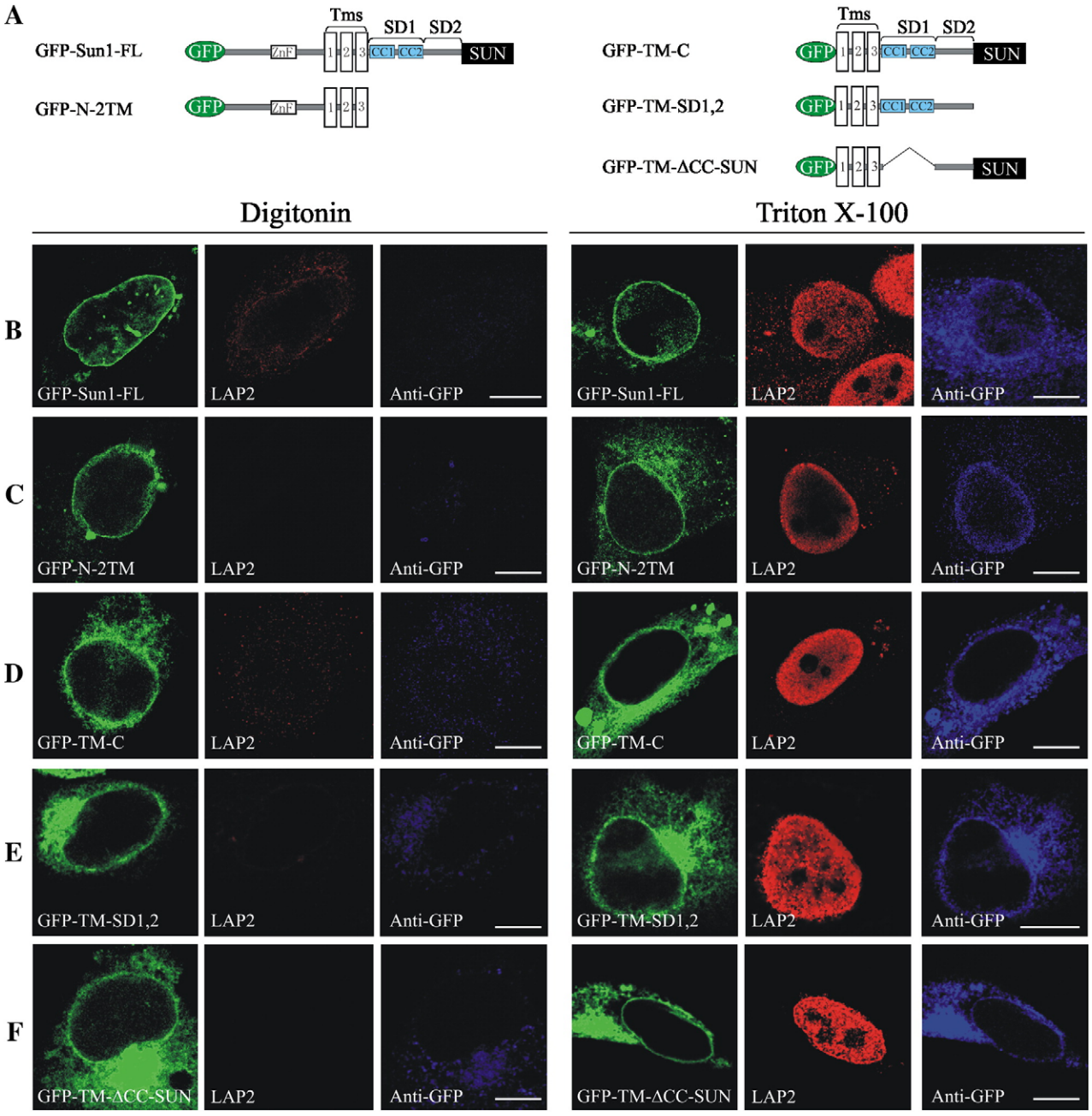

Fig. 1. GFP-tagged Sun1 variants localize specifically to the INM. (A) Schematic of GFP-Sun1-FL, GFP-N-2TM, GFP-TM-C, GFP-TM-SD1, 2 and GFP-TM-ΔCC-SUN. FL: full-length; ZnF: zinc finger; TMs: transmembrane domains; CC: coiled-coil domain; SUN: *S*ad1/*UNC*-84 homology domain; SD1: subdomain 1; SD2: subdomain 2. The topology of ectopically expressed Sun1-constructs was evaluated by selective permeabilization of HeLa cells subjected to direct and indirect immunofluorescence. (B-F) GFP-Sun1-FL, GFP-N-2TM, GFP-TM-C, GFP-TM-SD1, 2 and GFP-TM-ΔCC-SUN transfected HeLa cells were permeabilized with either digitonin or Triton X-100 and stained with GFP antibodies. LAP2 counter-staining was used as control. Bars = 10 μm.

(64 kDa) and tetramers (128 kDa). The BSA control migrates as a monomer under the same conditions. The purified Sun1 SD1, 2 proteins were subjected also to cross-linking using various concentrations of glutaraldehyde and analyzed by SDS-PAGE. Without glutaraldehyde treatment, only the monomer band was observed, whereas, in the cross-linked SD1, 2 protein samples, additional dimer and tetramer bands became evident. Furthermore, the relative amount of the monomer decreased and shifted towards higher order structures, which did not enter the gel, by increasing the amount of the cross-linking reagent (Fig. 3C). In contrast, no higher molecular mass polypeptides were detected in the glutaraldehyde treated BSA samples (data not shown). In summary, our data indicate that the SD1, 2 domains can form dimers and tetramers in vitro.

To narrow down the Sun1 self-interacting sequences, we performed GST pull-down assays. For this we fused GST to the SD1-domain (GST-SD1) to pull-down ectopically expressed GFP-SD1,2 fusion proteins from COS7 cell lysates (Fig. 3D). The GFP-SD1,2 fusions lack the transmembrane domains and localize diffusely in the cytoplasm (data not shown). As anticipated, GST-SD1 was able to precipitate GFP-SD1,2 from COS7 cell lysates. In contrast, no interaction with GFP-SD1,2 was observed for GST alone (Fig. 3D). To exclude the binding between SD1 and SD2, we constructed GFP-SD2. As shown in Fig. 3D, we could not detect an interaction between GST-SD1 and GFP-SD2.

To confirm the proposed oligomerization potential of both the mouse and human Sun1 coiled-coil domains also in vivo we

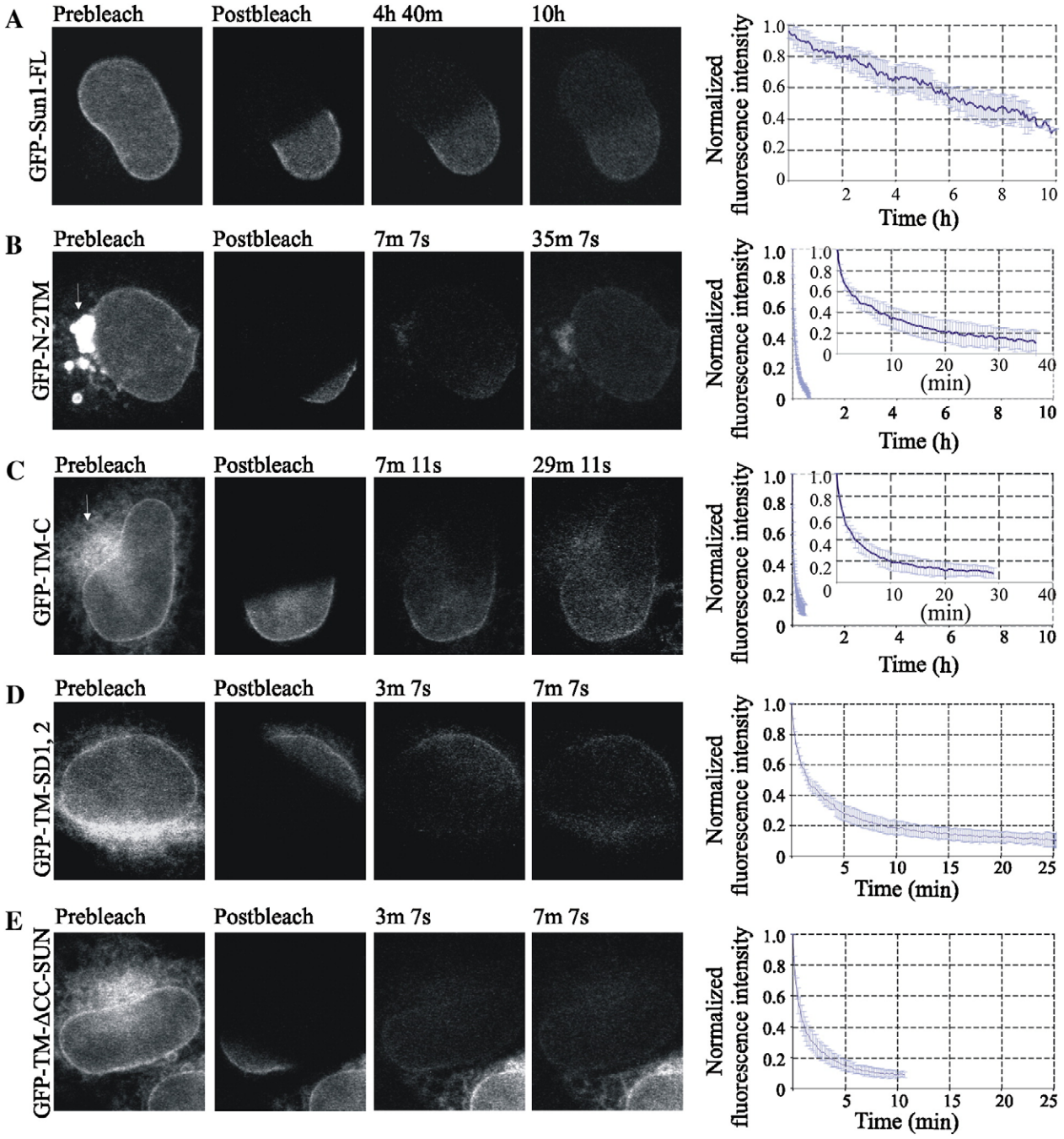

Fig. 2. Sun1 is an immobile NE protein. (A–E) HeLa cells expressing GFP-Sun1-FL, GFP-N-2TM, GFP-TM-C, GFP-TM-SD1, 2 or GFP-TM-ΔCC-SUN were imaged before and after photobleaching of the entire nucleus with the exception of a small NE region. Arrows indicate the accumulation of the GFP-fusions in the ER. Corresponding plots for fluorescence decay kinetics with standard deviation from the unbleached region of iFRAP experiments are shown on the right side. Insets depict the early dynamics at a standardized time scale of 40 min. At least 4 experiments were performed for each GFP-fusion and used to deduce the standard deviation.

performed a yeast two-hybrid system analysis. For that, the respective coiled-coil domains were fused either with GAL4 DNA-binding domains in the pGBKT7 vectors (BD-mSD1, 2, residues 432–737; BD-hSD1, residues 404–493) or the GAL4 transcription activation domains in the pGADT7 vectors (AD-mSD1, 2, residues 432–737; AD-hSD1, residues 404–493), respectively. Fig. 3E shows that cells cotransformed with pGADT7-mSD1, 2 and pGBKT7-mSD1, 2, or pGADT7-hSD1 and pGBKT7-hSD1 grew on the selection plates and were positive in the β-galactosidase test. No interaction was detected in negative controls. Conclusively, our studies clearly indicate that mammalian Sun1 forms homo-oligomers through its SD1-domains.

3.4. Sun1 oligomers contain interchain disulfide bonds

To gain further insights into Sun1 oligomerization, we next focused our studies on the full-length Sun1 protein. We transfected C-terminal V5-tagged full-length human Sun1 into COS7 cells and analyzed the cell lysates by anti-V5 western blotting. Sun1 immunoblotting analysis indicated the presence of SDS-resistant dimers under non-reduced conditions. Without heating and in the absence of dithiothreitol (DTT) in the COS7 lysates, monomer, dimer and tetramer bands were detected even under high SDS concentrations (0.5%). In the presence of 100 mM DTT, however, dimer and higher molecular mass signals were abolished (Fig. 4A). Heating of the samples at 70 °C or 95 °C

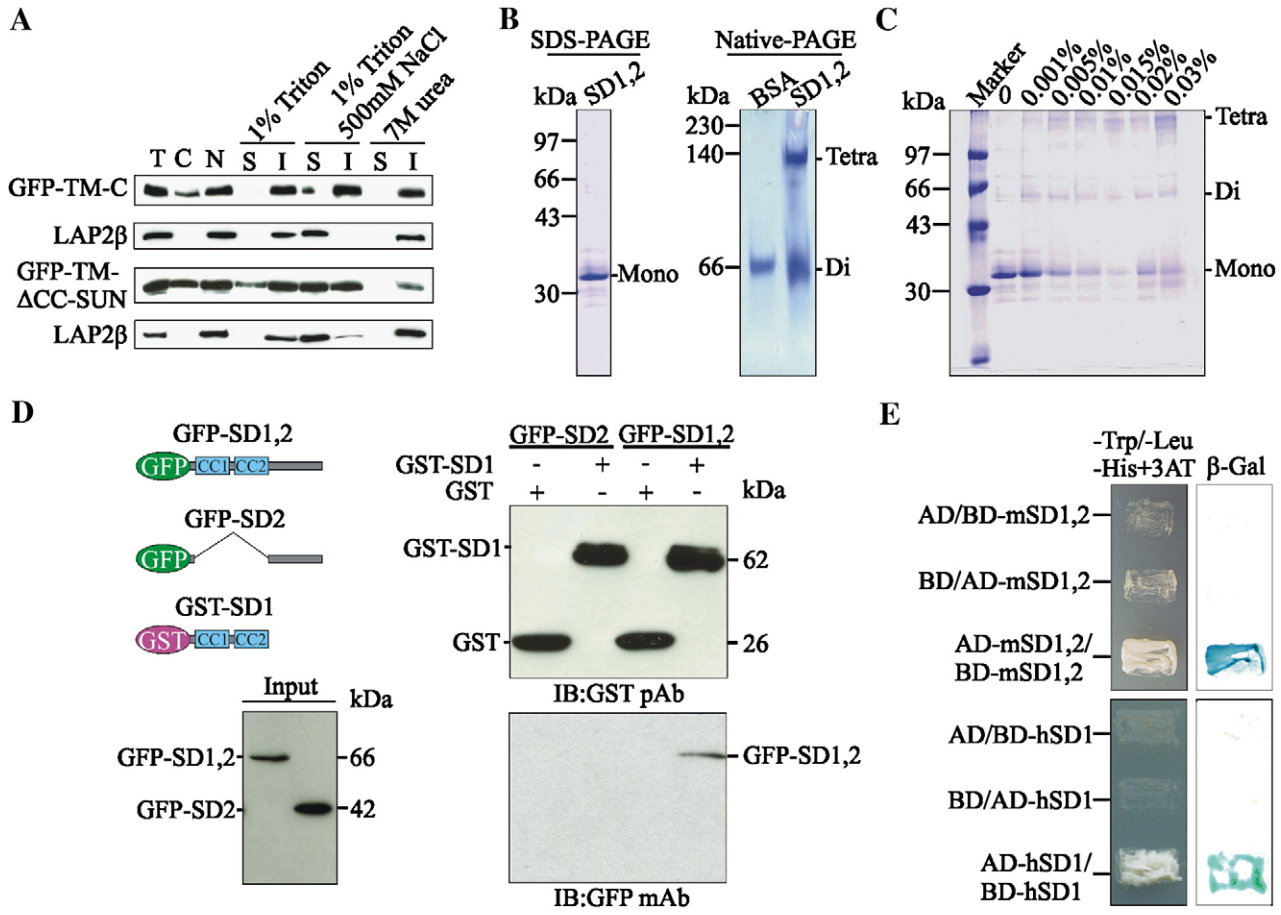

Fig. 3. The Sun1 C-terminal coiled-coil domain oligomerizes and stabilizes Sun1 at the NE. (A) Solubilization properties of GFP-TM-C and GFP-TM-ΔCC-SUN under various extraction conditions. Total (T), cytoplasmic (C) and nuclear (N) fractions were produced from GFP-TM-C or GFP-TM-ΔCC-SUN transfected COS7 cells. Nuclear fractions were extracted in buffers containing Triton X-100, Triton X-100 plus salt and urea, as indicated. Soluble (S) and insoluble (I) fractions were analyzed by western blotting using anti-GFP antibodies. The same lysates were analyzed for LAP2β. (B) Purified mouse Sun1 SD1, 2 fractions were supplemented with SDS-sample buffer containing β-mercaptoethanol and subjected to SDS-PAGE using a 12% SDS-polyacrylamide gel (left panel). The same purified SD1, 2 fractions and BSA (Bovine serum albumin) were supplemented with blue native sample buffer lacking SDS and β-mercaptoethanol. After electrophoresis on a 10% native polyacrylamide gel, the gel was visualized by Coomassie staining. Mono: monomer; Di: dimer; Tetra: tetramer. (C) Equal amounts of the purified mouse Sun1 SD1, 2 were cross-linked with different glutaraldehyde concentrations. Reactions were terminated by addition of SDS-sample buffer. The samples were loaded on a 12% SDS gel and stained by Coomassie Blue. (D) COS7 cells were transiently transfected with GFP-SD1, 2 and GFP-SD2, respectively. The cell lysates were analyzed by immunoblotting using anti-GFP antibodies (Input). COS7 cell lysates expressing the GFP-SD1, 2 or GFP-SD2 were incubated with beads coupled to GST-SD1 or GST. Specifically bound proteins were subjected to SDS-PAGE followed by anti-GST western blotting. The same membrane was later stripped and submitted to anti-GFP immunoblotting. (E) Yeast two-hybrid assays demonstrate that the coiled-coils of both mouse and human Sun1 interact with each other. Empty BD and AD plasmids were used as negative controls. Y190 yeast cells were cotransformed with AD/BD-mSD1, 2, BD/AD-mSD1, 2, AD-mSD1, 2/BD-mSD1, 2, or AD/BD-hSD1, BD/AD-hSD1, AD-hSD1/BD-hSD1. The interaction was monitored by growth on SD-Trp-Leu-His (60 mM 3AT) plates. X-Gal assays were also performed to confirm the interaction. AD: GAL4 activation domain; BD: GAL4 DNA-binding domain.

resulted in a decrease of the monomeric signal intensity, through an irreversible Sun1-V5 aggregation (arrow in Fig. 4A), a known effect for some transmembrane proteins [39]. Similar results were also obtained for endogenous Sun1 proteins (Fig. S2A, asterisk).

The presented data strongly suggested the existence of disulfide bridges between Sun1 molecules. Therefore, we next examined the primary structures of mouse and human Sun1 for cysteines. As depicted in Fig. 4B and C, four conserved cysteine residues are present in both human and mouse Sun1 C-termini. One is located in the SD2 domain (human Sun1 Cys^{526}), the other three (human Sun1 Cys^{657}, Cys^{695} and Cys^{800}) are located in the SUN-domain.

In order to identify which cysteines were sufficient to mediate the formation of disulfide-linked oligomers, four additional constructs were made. Human Sun1 TMC-HA (residues 240–812) containing all four conserved cysteins (Cys^{526}, Cys^{657}, Cys^{695}, Cys^{800}) in the SD2/SUN-domains, and TMSD1, 2-HA (residues 240–632), which lacks the SUN-domain and contains only the SD2 domain Cys^{526}. We also generated TMC C/A-HA in which Cys^{526} was replaced by an alanine and TMSD1, 2 C/A-HA, which contains the same C526A mutation and lacks the SUN-domain (Fig. 4C). The constructs were transiently transfected in COS7 cells and lysed with RIPA buffer containing 0.1% SDS and either 100 mM iodoacetamide (IA) or 20 mM NEM to prevent artificial disulfide bond formation. The lysates were submitted to non-reduced or reduced conditions, respectively. Equal amount of protein from each sample was loaded on a 12% gel, analyzed by SDS-PAGE and concomitant anti-HA western blotting. In the absence of DTT, bands corresponding to Sun1-dimers were detectable in the absence or presence of 0.5% SDS in TMC-HA or TMSD1, 2-HA lysates. However, in the presence of DTT, dimer bands were completely absent (Fig. 4D). Replacing Cys^{526} by an alanine completely abolished the dimer formation of TMC C/A-HA or TMSD1, 2 C/A-HA (Fig. 4D), respectively. SUN-domain cysteines are therefore not involved in this process, whereas the SD2 domain resident Cys^{526} might contribute to the formation of Sun1 oligomers.

To address the biological relevance of the Sun1 interchain disulfide bridge in Sun1 NE dynamics, we transiently transfected GFP-TMC and GFP-TMC C/A in HeLa cells and performed iFRAP analysis on the transfected cells. Four individual cells for each construct were followed. However, no significant differences were observed between these two constructs (Fig. 5), suggesting that the disulfide bond

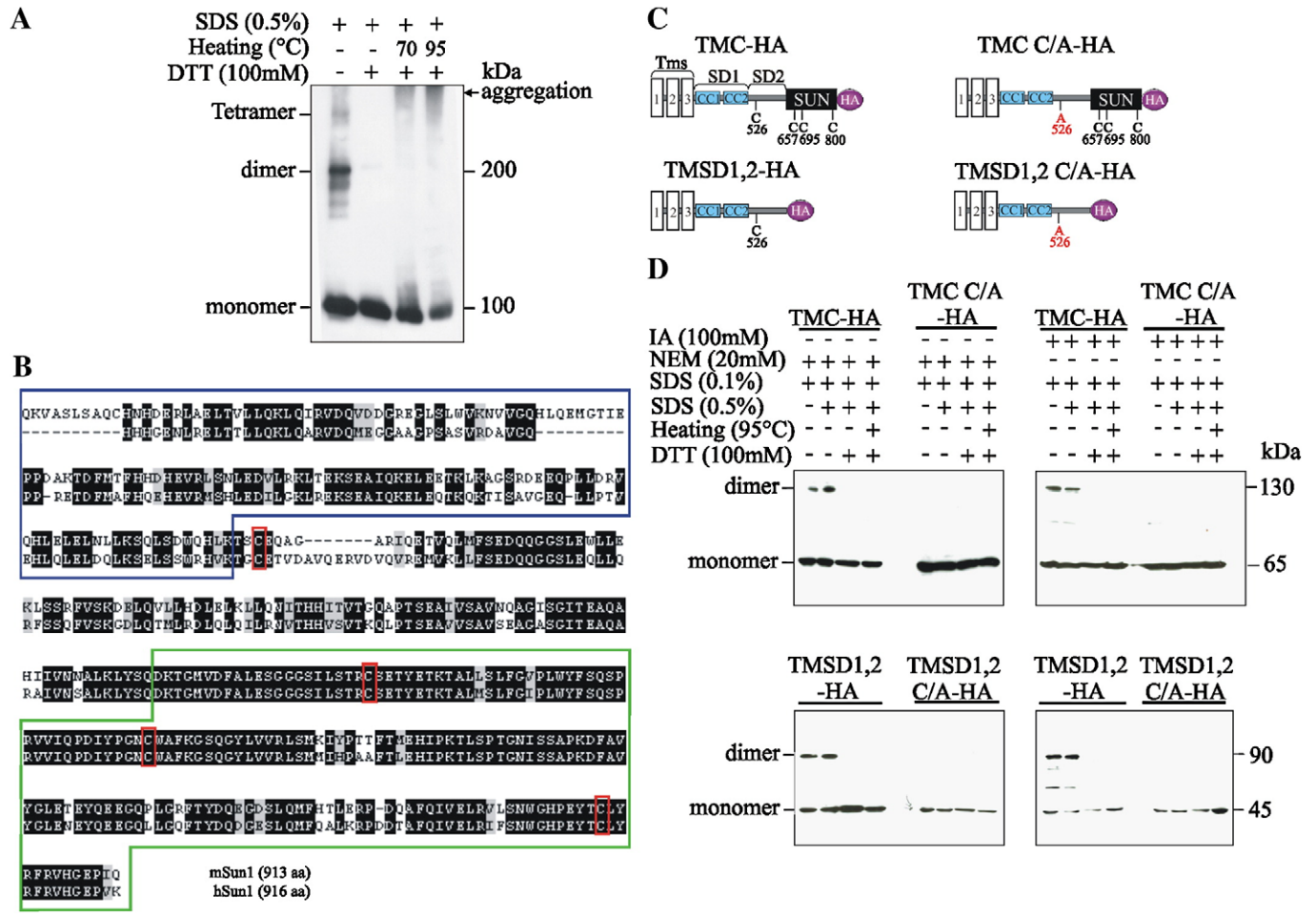

Fig. 4. Sun1 oligomers contain interchain disulfide bonds formed via C-terminal cysteines. (A) Sun1-V5 was transiently transfected in COS7 cells. RIPA-buffer cell lysates were prepared and divided into four equal portions, and treated under different experimental conditions as indicated on the top of the blot. Lysates were resolved by 6% SDS-PAGE and detected by anti-V5 immunoblotting analysis. (B) Alignment of the mouse and human Sun1 C-terminus. Identical residues and conservative substitutions are shown in black (Cysteines: marked by red frame) and gray, respectively. Mouse and human Sun1 coiled-coil domains: blue frame; SUN-domains: green frame; SD2 domain: unboxed area. (C) Schematic of the human Sun1 TMC-HA and TMSD1, 2-HA fusion proteins, and the point mutated TMC C/A-HA and TMSD1, 2 C/A-HA. Major Sun1 domains are depicted and the conserved cysteines in SD2 and SUN-domains are indicated below the schematic. In TMC C/A-HA and TMSD1, 2 C/A-HA the SD2 resident cysteine was mutated to an alanine (red). (D) COS7 cells were transiently transfected with TMC-HA, TMSD1, 2-HA, TMC C/A-HA or TMSD1, 2 C/A-HA. Cell lysates containing either 100 mM IA or 20 mM NEM were treated under different experimental conditions as indicated on the top of the western blots and detected by anti-HA western blotting. Both TMC-HA and TMSD1, 2-HA chimeric proteins yield dimers in the absence of DTT. No dimers were formed in TMC C/A-HA or TMSD1, 2 C/A-HA cell lysates in the presence of DTT.

between the Sun1 lumenal segments does not play a major role in the Sun1 C-terminal domain NE turnover dynamics, although from our interaction data we are prompted to assign a stabilizing function to interchain disulfide bonding for the full-length Sun1 protein.

3.5. Sun1 provides a stable platform for multiple macromolecular assemblies

Our data so far show that Sun1 molecules oligomerize and form stable complexes with itself at the NE. In order to verify this, we next performed an indirect immunofluorescence analysis of endogenous Sun1 proteins in HeLa cells. Confocal microscopy clearly indicated the organization of Sun1 into clustered assemblies at the NE (Fig. 6A′). We confirmed this further by employing two new Sun1 antibodies (Sun1A and Sun1B, characterized in Fig. S2). As indicated these new antisera also recognized a clustered Sun1 pattern at the NE surface, highly reminiscent of NPC staining (Fig. 6B, B′; similar results obtained in other cell lines, such as HaCaT, COS7, Ramos, SW480-data not shown). Co-staining with the NPC marker mAb414 revealed a pool of Sun1 that concentrated in the vicinity or overlapped with NPCs (Fig. 6A″, B and B′ notched arrows in the insets). This result is in agreement with Liu et al. [26], who demonstrated that NPCs colocalize with ectopically expressed GFP-tagged Sun1. Interestingly, a second pool of endogenous Sun1 structures also became evident, which did not colocalize with NPCs (Fig. 6A″, B and B′ arrows in the insets). Similar results were observed in other cell lines, although the percentage of Sun1-NPC overlapping entities varied, most likely due to the metabolic status or the cell cycle status of the cells (data not shown). Moreover, ectopic expression of Sun1 full-length constructs indicated also the presence of two distinct NE Sun1 topologies (data not shown). One fraction of Sun1 foci colocalizes with NPCs, whereas the second appears distinct from NPCs. A newly developed antibody recognizing mammalian Sun2 (characterized in Fig. S2) was then used to investigate the association of Sun2 with NPCs. Endogenous Sun2, like observed for Sun1, also displayed a clustered appearance at the NE surface. As already suggested by Liu et al. [26] endogenous Sun2 antigenic clusters were almost absent at sites of nuclear pores (Fig. 6B″). These results and already presented data on a possible Sun1/2 interaction [27] prompted us to investigate the possibility that Sun2 assemblies at the NE could be identical with Sun1 antigenic assemblies, which did not overlap with the NPC.

Unfortunately no monoclonal antibodies to any of Sun1 or Sun2, respectively, are available and we had to analyze local interactions by examination of endogenous Sun1 in Sun2-V5 transfected HaCaT cells. As shown in Fig. 7A–A″, a large Sun1 proportion colocalizes with Sun2

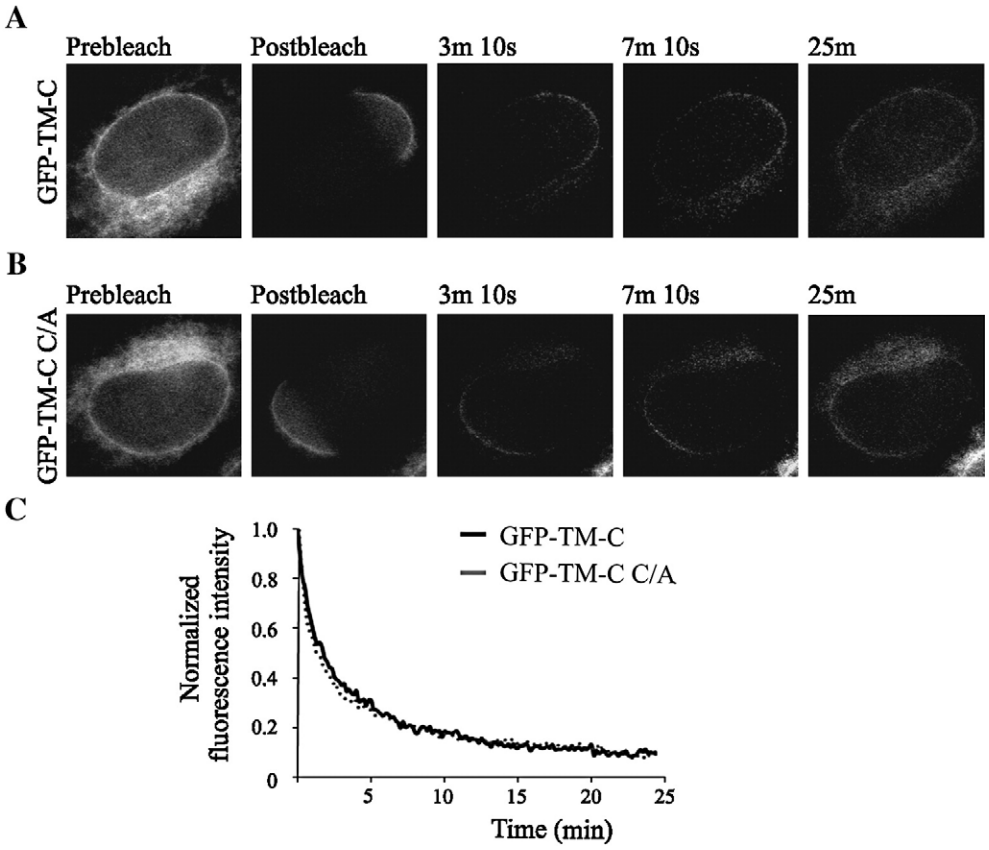

Fig. 5. The SD2 domain interchain disulfide bond does not contribute to the immobility of Sun1 C-terminal segments. (A, B) Selected time points from a HeLa cell example expressing GFP-TMC or GFP-TMC C/A, imaged before and after photobleaching of the Sun1 signal except for a small NE region. (C) Plots of the fluorescence decay kinetics of the unbleached region for the mutant (dashed black curve) and the GFP-TMC (black curve). The curves are the average of four different cells.

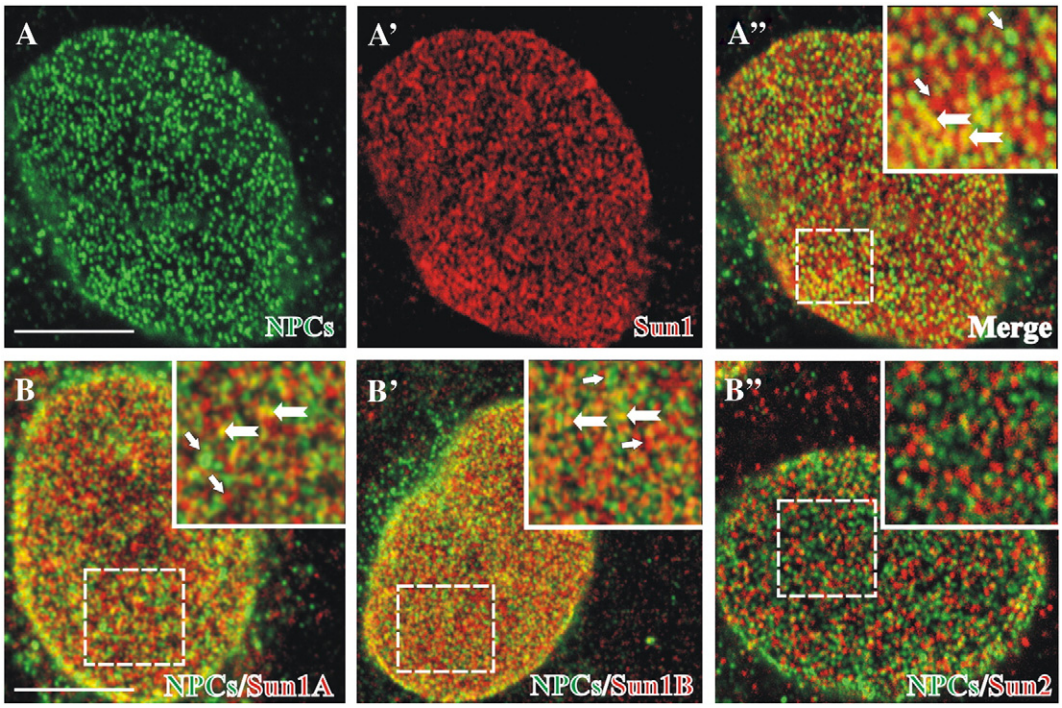

Fig. 6. NPCs colocalize with Sun1 but not Sun2. (A–B′) Confocal sections of the lower surface of HeLa cell nuclei. Cells were double labeled with anti-NPCs (A, A″, B, B′ in green) and three specific anti-Sun1 (A′, A″, B, B′ in red) antibodies. The optical surfaces of nuclei are shown with enlargements of the regions indicated. Sun1 positive spots colocalized with NPCs are indicated with notched arrows. Sun1 and NPCs positive structures distinct from each other are represented by arrows. (B″) The equatorial optical section from the HeLa cell nucleus was double labeled with NPCs (in green) and Sun2 (in red). The majority of Sun2 does not colocalize with NPCs. Bars = 10 μm.

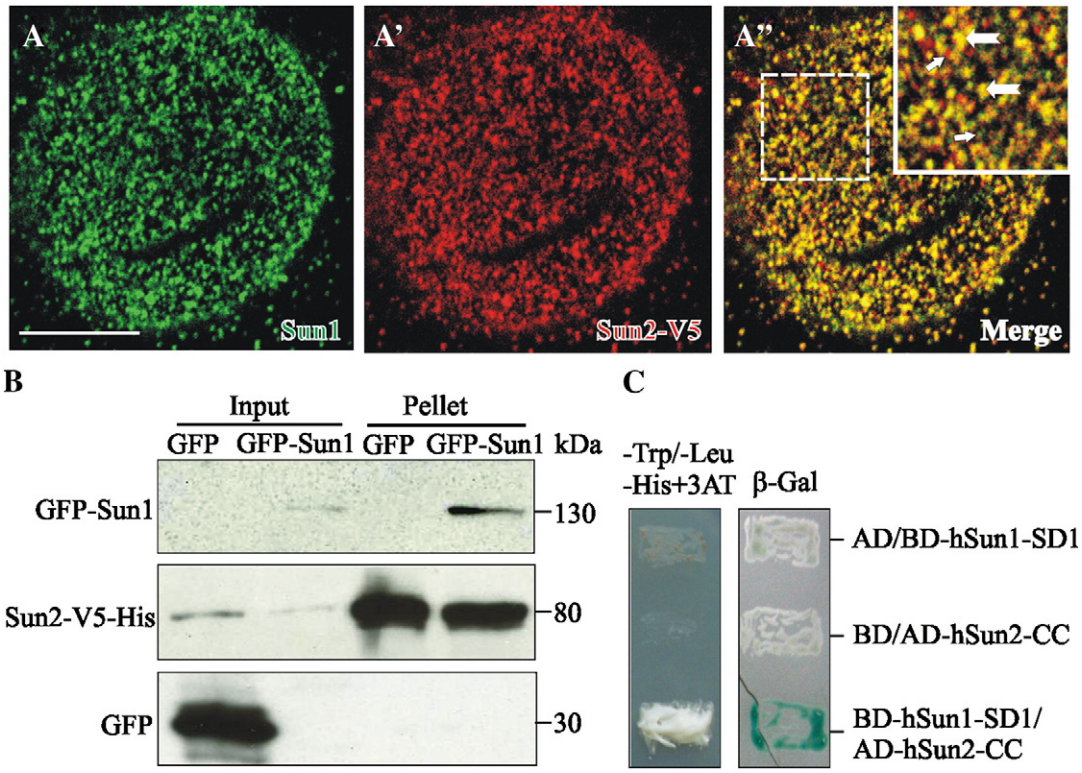

Fig. 7. Sun1 and Sun2 proteins heterodimerize through their respective coiled-coil domains and certain Sun1/2 complexes colocalize at the NE. (A–A″) Immunofluorescence analysis of HaCaT cells expressing Sun2-V5 indicates a significant overlap between Sun1 and Sun2 positive structures (notched arrows). Sun1 and Sun2 staining patterns which do not colocalize with each other are indicated with arrows. Bar = 10 μm. (B) His-pull-down assays of COS7 lysates (Input) expressing GFP-Sun1 and Sun2-V5-His or GFP and Sun2-V5-His proteins. Ni-NTA bound proteins were analyzed by SDS-PAGE and anti-GFP and anti-V5 western blotting. GFP-Sun1 was pulled down by Sun2-V5-His. GFP alone did not interact with Sun2-V5-His. (C) The coiled-coil domains of Sun1 and Sun2 interact in vivo in yeast cells. The corresponding plasmids were cotransformed into yeast cells and assessed for growth and by the filter lift β-galactosidase assay. Empty binding domain vector pGBKT7 or activation domain vector pGADT7 was cotransformed with pGADT7-hSun2-CC or pGBKT7-hSun1-SD1, respectively. AD: activation domain; BD: DNA-binding domain; CC: coiled-coil.

(notched arrows in the inset), whereas in some areas within the same nucleus the Sun1 and Sun2 patterns appear distinct (arrows in the insets). Similar observations were obtained in the vice-versa setup, when we examined endogenous Sun2 in Sun1-V5 expressing cells using Sun2 specific antibodies (also in HeLa cells, data not shown). The colocalization of the Sun1/Sun2 structures is in agreement with current literature indicating that Sun2 proteins form heterodimers with Sun1 molecules [27]. Inspired by these facts, we went ahead to address in more detail the ability of Sun2 to heterodimerize with Sun1. For this, GFP-tagged human Sun1 full-length and V5-His-tagged human Sun2 full-length were transiently cotransfected in COS7 cells. The cell lysates were incubated with Ni-NTA agarose beads to pull-down exogenous Sun2. Bound proteins were then analyzed by SDS-PAGE and subjected to western blotting using GFP antibodies. As a negative control we used GFP, which was cotransfected with Sun2-V5-His into COS7 cells. As shown in Fig. 7B, ectopically expressed GFP-Sun1 and Sun2-V5-His were successfully expressed in cotransfected cell lysates (Input). In contrast to GFP, however, only GFP-Sun1 was specifically pulled down with the Sun2-V5-His protein (Pellet). In order to identify the respective domains involved in the Sun1/Sun2 association in vivo, we performed yeast two-hybrid analysis. The coiled-coil domain of human Sun1 (hSun1-SD1, residues 404–493) was cloned into pGBKT7 vector and the coiled-coil domain of human Sun2 (hSun2-CC, residues 400–505) was cloned into pGADT7 vector. When pGBKT7-hSun1-SD1 and pGADT7-hSun2-CC plasmids were cotransformed in the Y190 yeast strain, an interaction between these two proteins was observed in both growth and β-galactosidase activity assays (Fig. 7C). Neither growth, nor β-galactosidase activity was detected in negative controls using pGBKT7-hSun1-SD1 with pGADT7 or pGADT7-hSun2-CC with pGBKT7.

These data together assert that a subset of Sun1 and Sun2 molecules interact directly with each other at the INM through their respective coiled-coil segments. Moreover, they also imply the existence of distinct SUN-protein complexes. Our data would clearly point to a model, where highly immobile Sun1 complexes form a stable platform for associations with more dynamic molecules, probably also based on a functional necessity. Therefore, it would be interesting to investigate in the near future whether distinct cellular functions can be assigned to specific SUN-domain protein assemblies at the NE.

4. Discussion

In the current study we characterized in more detail the murine Sun1 dynamics and expanded current data regarding its NE-localization properties. The implemented iFRAP experiments indicate that full-length Sun1 is among the most immobile INM proteins described to date. A low lateral mobility has also been reported in human Sun1 (UNC84A) FRAP experiments [26,28] monitored, however, for a limited time period (up to 800 s). In our iFRAP experiments we were able to follow the photobleached GFP-Sun1 expressing cells up to 10 h and still no complete equilibration was reached within the bleached area. The dynamics of many NE proteins has been characterized by fluorescence recovery after photobleaching (FRAP) assays. Lamin A was shown to move back into the bleach area very slowly, similar to that reported for lamin B1 (>180 min) [40]. GFP-tagged lamin C expressed in CHO cells has also been reported to show very little recovery after 1 h [41]. Most INM proteins such as emerin, LAP2β, and MAN1 are dynamic, having recovery halftimes of about 1 min [42]. LBR is more immobile at the NE. More than 60% LBR-GFP

fractions reside within the NE membranes 10 min after photobleaching [43]. The extensive immobilization of GFP-Sun1 suggests a tight binding to fixed structural components of the nucleus or/and retention by assembly into multimeric complexes, which would be expected to result in low diffusion rates. GFP labeled nuclear pore complex components for example, which are known to form oligomeric complexes have been shown to diffuse slowly within the NE [31,44].

Our data do not assign a major role for the SUN-domain itself in the Sun1 dynamics. They rather suggest important roles for the Sun1 coiled-coil domain, through which Sun1 forms dimers. Genetic evidence indicates that *C. elegans* UNC-84 exists as dimers at the NE [45] similar to matefin, another SUN-domain protein in *C. elegans* reported to homodimerize [21]. Sun-1 in *D. discoideum* also forms oligomers via the C-terminal coiled-coil domains [19]. Sun2 forms also homodimers through the N-terminal region and the coiled-coil domains [27]. These data together suggest that oligomerization at the NE is a common feature for SUN-family members.

The lumenal domain of Sun1 has been suggested to permit homo-oligomerization [26,27]. We were able to narrow down the oligomerization domain to the coiled-coil region (SD1-domain). Furthermore, this Sun1 C-terminal region resides in the PNS, which is a part of the ER lumen. Unlike the cytoplasm, the ER provides an oxidizing environment favoring disulfide bond formation [46,47]. Indeed, V5-tagged full-length Sun1 has the ability to form SDS-resistant dimers and tetramers under non-reduced conditions. Mutagenesis assays demonstrated that the cysteine residue (Cys^{526}) in the Sun1 SD2 domain, adjacent to the C-terminal border of the coiled-coil region, is responsible for the formation of the disulfide bond. Thus, Sun1 homo-oligomers form through coiled-coil interactions and interchain disulfide bonds (Fig. 8). We also tested the dynamics of GFP-tagged TM-C and TMC C/A by iFRAP analysis. However, no significant differences were observed between these two constructs, suggesting that the disulfide bond between the Sun1 lumenal segments does not contribute to the Sun1 immobility in the PNS. Nonetheless, we cannot exclude that such associations may exhibit important stabilizing functions in the full-length Sun1 protein. It is also interesting to note that the cysteine residue forming the disulfide bond resides within the major Nesprin binding site of Sun1 [11]. Therefore, the interchain disulfide bonds formed among Sun1 molecules may affect the structural conformation of Sun1 complexes and consequently influence interactions to its binding partners. Clearly, additional studies are required to reveal potential roles for the disulfide bonds in the Sun1 biology.

We also demonstrated that Sun1 interacts with Sun2 through their respective coiled-coil domains. This finding is further underlined by our data indicating that a substantial fraction of Sun1 molecules colocalize with the Sun2 structures. The dynamic rigidity of Sun1 containing complexes urged us to investigate a potential association to NPCs. Colocalization studies revealed that a significant portion of Sun1 molecules colocalized to NPCs in HeLa cells. In contrast, Sun2 localization was clearly distinct from NPC sites. Similar data have recently been shown by Liu et al., which suggest a close association of GFP-tagged Sun1 with nuclear pore complexes [26]. Our data, however, suggest in addition the existence of a second Sun1 pool that is clearly distinct from NPCs. Based on our immunofluorescence stainings our assumption is that a large fraction of these particular complexes may constitute Sun1 and Sun2 oligomers (Fig. 8). However, we cannot exclude the presence of Sun1 homophilic complexes within this second Sun1 fraction. In summary, our data suggest that SUN-proteins can form higher ordered complexes at the NE, constituting multiple docking sites for other proteins.

The oligomerization of Sun1 may be important for its function at the NE. Notwithstanding that finding, the existence of a variety of several independent, individual SUN-protein containing complexes can be assumed. It can further be envisaged that members of the SUN-protein superfamily are functionally redundant, exemplified by the finding that Sun1 knockout mice only show defects in gametogenesis, most likely as a result from failures in telomere attachment during meiosis [24]. Particularly interesting is the fact, that testis-specific isoforms exist for mammalian Sun1, which cannot be replaced functionally by other Sun1 isoforms [26] or even members of the SUN-superfamily (Gotzmann et al., unpublished data). Each SUN-complex could directly anchor two or more binding partners and thereby significantly enhance or modulate the mechanical stability of the protein complexes that bridge the NE.

Strikingly, the immobile Sun1 features are only realized when both Sun1 nucleoplasmic and perinuclear segments were present.

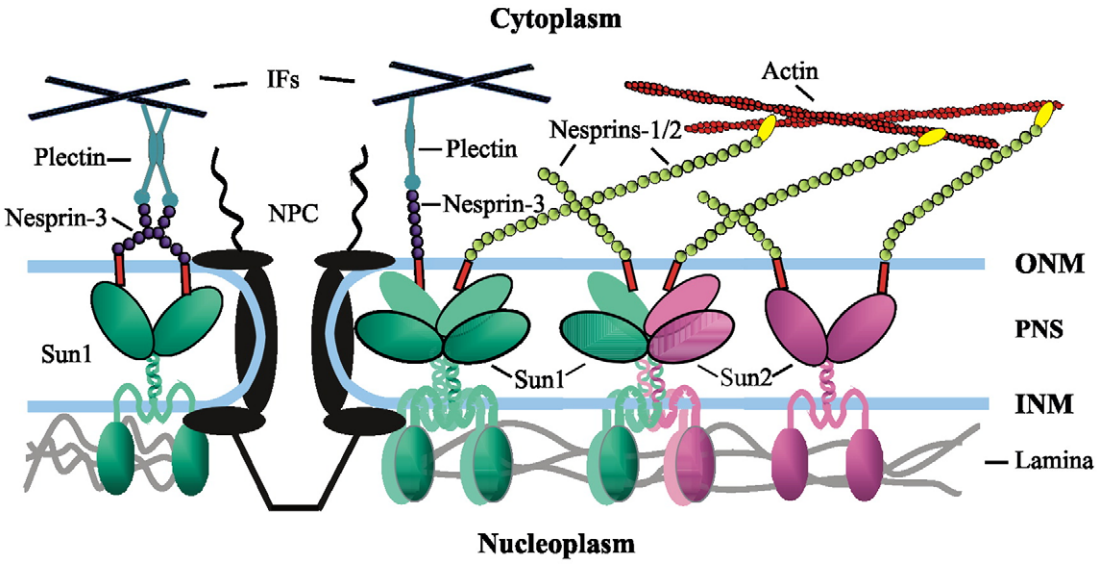

Fig. 8. Model illustrating that SUN- and KASH-domain proteins form higher ordered NE complexes. Sun1 (green) and Sun2 (pink) can form dimers via the coiled-coil domains at their C-termini. Sun1 and Sun2 also can form tetramers or higher oligomers through their coiled-coil domains, which may be further linked by Sun1 interchain disulfide bridges formed in the PNS. Nesprin-1/-2/-3 isoform homotypic self-interactions may further contribute to Sun1/2 oligomer expansion. Thus, SUN-KASH complexes may form higher ordered ONM tethering platforms, allowing the uniform integration of the nuclear surface to the cytoskeleton. ONM: outer nuclear membrane; PNS: perinuclear space; INM: inner nuclear membrane; NPCs: nuclear pore complexes; IFs: intermediate filaments.

Several possibilities may account for this result. First, Sun1 N- and C-termini could bind to distinct NE-associated proteins that contribute collectively to its NE retention. This scenario is plausible, considering that Sun1 domains are clearly distinct in their primary structure and more importantly in their topology. In line with the above is that the Sun1 N-terminus interacts with lamin A, although its NE localization seems to be largely independent from the presence of A-type lamins [10,11]. The Sun1 N-terminus is also capable of self-association, a feature potentially required for association with DNA [27,29]. Most recent data also point to an involvement of N-terminal domains of Sun1 in the degree of chromosome compaction after mitosis [25]. The presence of a variety of N-terminal splicing isoforms may account for differences in the binding spectrum for lamins and/or chromatin [26]. Moreover, the mouse Sun1 nucleoplasmic segment contains a Zinc-finger motif, which associates with DNA, whereas the C-terminus associates with the Nesprin-1/-2/-3 KASH-domains.

The second possibility is that Sun1 N-terminal association to its binding partners has immediate structural effects on the C-terminus. Binding for example to the nuclear lamina or/and chromatin may unfold the C-terminus in such a way, so that inter- or intra-molecular interactions are modulated. If this holds true, signals from the nucleus may be efficiently transmitted to the cytoplasm and vice-versa. Support for this attractive model comes from the fact that while GFP-TM-C interacts with the endogenous Sun1 in vitro, its NE lateral mobility is clearly reduced when compared to the Sun1 full-length protein. Additional experiments are needed to validate all those thoughts. Thus, the combined oligomerization capacity of the Sun1 N- and C-termini may account for the dramatic immobility of the full-length Sun1 protein.

Current data also suggest that the biochemical properties of SUN and KASH-domain proteins may jointly organize these molecules into complexes. In fact Nesprin molecules themselves may contribute to an expansion and the formation of larger macromolecular complexes (Fig. 8). Nesprin-1 was shown to oligomerize with itself through its C-terminal spectrin repeats [48]. Nesprin-2 giant isoforms function as NE guardian molecules that tether smaller Nesprin-2 C-terminal isoforms at the ONM [49,50]. Also, Nesprin-3 oligomerizes with itself through its N-terminal spectrin repeats [51]. Hetero-oligomerization aspects among Nesprins-1/-2/-3 have not been examined so far; we cannot exclude, however, the possibility that Nesprins may form a filament network by their own at the ONM and contribute also to the immobility of Sun1 at the NE. The fact that Sun1/2 oligomerize suggests that such an assembly may structurally and functionally integrate various KASH-domain containing proteins within these complexes. This view is further supported by a recent report demonstrating that mammalian KASH-proteins interact promiscuously with Sun1/2 proteins [52].

Collectively these thoughts indicate that more research is needed to shed light in a new cell biological area governing the structural and functional integration of cytoplasmic and nuclear compartments.

Acknowledgements

This work was supported by grants from the Knut and Alice Wallenberg foundation to C.S. and M.U., from the “Hochschuljubiläumsstiftung der Stadt Wien” and a collaborative project support from the Knut and Alice Wallenberg foundation to J.G.; from the Austrian Science Research Fund (FWF P17871) and the EURO-Laminopathies research project of the European Commission (Contract LSHM-CT-2005-018690) to R.F.; from the German Research Council (DFG EL 246/3-1) to J.E.; a postdoctoral fellowship from the Human Science Foundation (HFSP) to L.S.; from the CMMC to A.A.N.; from the NRW International Graduate School (IGS) in Genetics and Functional Genomics to W.L.; from the DFG (KA 2778/1-1) and a Wellcome Trust ‘Value in People’ award to I.K.

Appendix A. Supplementary data

Supplementary data associated with this article can be found, in the online version, at doi:10.1016/j.bbamcr.2008.09.001.

References

[1] L. Gerace, B. Burke, Functional organization of the nuclear envelope, Annu. Rev. Cell Biol. 4 (1988) 335–374.
[2] D. Gorlich, U. Kutay, Transport between the cell nucleus and the cytoplasm, Annu. Rev. Cell Dev. Biol. 15 (1999) 607–660.
[3] I.G. Macara, Transport into and out of the nucleus, Microbiol. Mol. Biol. Rev. 65 (2001) 570–594.
[4] B. Burke, J. Ellenberg, Remodelling the walls of the nucleus, Nat. Rev., Mol. Cell Biol. 3 (2002) 487–497.
[5] N. Stuurman, S. Heins, U. Aebi, Nuclear lamins: their structure, assembly, and interactions, J. Struct. Biol. 122 (1998) 42–66.
[6] J.L. Broers, F.C. Ramaekers, G. Bonne, R.B. Yaou, C.J. Hutchison, Nuclear lamins: laminopathies and their role in premature ageing, Physiol. Rev. 86 (2006) 967–1008.
[7] D.A. Starr, J.A. Fischer, KASH 'n Karry: the KASH domain family of cargo-specific cytoskeletal adaptor proteins, BioEssays 27 (2005) 1136–1146.
[8] Y.B. Tzur, K.L. Wilson, Y. Gruenbaum, SUN-domain proteins: ‘Velcro’ that links the nucleoskeleton to the cytoskeleton, Nat. Rev., Mol. Cell Biol. 7 (2006) 782–788.
[9] K. Wilhelmsen, M. Ketema, H. Truong, A. Sonnenberg, KASH-domain proteins in nuclear migration, anchorage and other processes, J. Cell Sci. 119 (2006) 5021–5029.
[10] M. Crisp, Q. Liu, K. Roux, J.B. Rattner, C. Shanahan, B. Burke, P.D. Stahl, D. Hodzic, Coupling of the nucleus and cytoplasm: role of the LINC complex, J. Cell Biol. 172 (2006) 41–53.
[11] V.C. Padmakumar, T. Libotte, W. Lu, H. Zaim, S. Abraham, A.A. Noegel, J. Gotzmann, R. Foisner, I. Karakesisoglou, The inner nuclear membrane protein Sun1 mediates the anchorage of Nesprin-2 to the nuclear envelope, J. Cell Sci. 118 (2005) 3419–3430.
[12] P.J. Stewart-Hutchinson, C.M. Hale, D. Wirtz, D. Hodzic, Structural requirements for the assembly of LINC complexes and their function in cellular mechanical stiffness, Exp. Cell Res. 314 (2008) 1892–1905.
[13] C.J. Malone, L. Misner, N. Le Bot, M.C. Tsai, J.M. Campbell, J. Ahringer, J.G. White, The *C. elegans* hook protein, ZYG-12, mediates the essential attachment between the centrosome and nucleus, Cell 115 (2003) 825–836.
[14] M.D. McGee, R. Rillo, A.S. Anderson, D.A. Starr, UNC-83 IS a KASH protein required for nuclear migration and is recruited to the outer nuclear membrane by a physical interaction with the SUN protein UNC-84, Mol. Biol. Cell 17 (2006) 1790–1801.
[15] D.A. Starr, M. Han, Role of ANC-1 in tethering nuclei to the actin cytoskeleton, Science 298 (2002) 406–409.
[16] D.A. Starr, Communication between the cytoskeleton and the nuclear envelope to position the nucleus, Mol. Biosyst. 3 (2007) 583–589.
[17] F. Miki, A. Kurabayashi, Y. Tange, K. Okazaki, M. Shimanuki, O. Niwa, Two-hybrid search for proteins that interact with Sad1 and Kms1, two membrane-bound components of the spindle pole body in fission yeast, Mol. Genet. Genomics 270 (2004) 449–461.
[18] S.L. Jaspersen, A.E. Martin, G. Glazko, T.H. Giddings Jr., G. Morgan, A. Mushegian, M. Winey, The Sad1-UNC-84 homology domain in Mps3 interacts with Mps2 to connect the spindle pole body with the nuclear envelope, J. Cell Biol. 174 (2006) 665–675.
[19] H. Xiong, F. Rivero, U. Euteneuer, S. Mondal, S. Mana-Capelli, D. Larochelle, A. Vogel, B. Gassen, A.A. Noegel, *Dictyostelium* sun-1 connects the centrosome to chromatin and ensures genome stability, Traffic 9 (2008) 708–724.
[20] K.K. Lee, D. Starr, M. Cohen, J. Liu, M. Han, K.L. Wilson, Y. Gruenbaum, Lamin-dependent localization of UNC-84, a protein required for nuclear migration in *Caenorhabditis elegans*, Mol. Biol. Cell 13 (2002) 892–901.
[21] A. Fridkin, E. Mills, A. Margalit, E. Neufeld, K.K. Lee, N. Feinstein, M. Cohen, K.L. Wilson, Y. Gruenbaum, Matefin, a *Caenorhabditis elegans* germ line-specific SUN-domain nuclear membrane protein, is essential for early embryonic and germ cell development, Proc. Natl. Acad. Sci. U. S. A. 101 (2004) 6987–6992.
[22] Y. Chikashige, C. Tsutsumi, M. Yamane, K. Okamasa, T. Haraguchi, Y. Hiraoka, Meiotic proteins bqt1 and bqt2 tether telomeres to form the bouquet arrangement of chromosomes, Cell 125 (2006) 59–69.
[23] I. Hagan, M. Yanagida, The product of the spindle formation gene sad1+ associates with the fission yeast spindle pole body and is essential for viability, J. Cell Biol. 129 (1995) 1033–1047.
[24] J. Schmitt, R. Benavente, D. Hodzic, C. Hoog, C.L. Stewart, M. Alsheimer, Transmembrane protein Sun2 is involved in tethering mammalian meiotic telomeres to the nuclear envelope, Proc. Natl. Acad. Sci. U. S. A. 104 (2007) 7426–7431.
[25] Y.H. Chi, K. Haller, J.M. Peloponese Jr., K.T. Jeang, Histone acetyltransferase hALP and nuclear membrane protein hsSUN1 function in de-condensation of mitotic chromosomes, J. Biol. Chem. 282 (2007) 27447–27458.
[26] Q. Liu, N. Pante, T. Misteli, M. Elsagga, M. Crisp, D. Hodzic, B. Burke, K.J. Roux, Functional association of Sun1 with nuclear pore complexes, J. Cell Biol. 178 (2007) 785–798.
[27] Q. Wang, X. Du, Z. Cai, M.I. Greene, Characterization of the structures involved in localization of the SUN proteins to the nuclear envelope and the centrosome, DNA Cell Biol. 25 (2006) 554–562.

[28] S. Hasan, S. Guttinger, P. Muhlhausser, F. Anderegg, S. Burgler, U. Kutay, Nuclear envelope localization of human UNC84A does not require nuclear lamins, FEBS Lett. 580 (2006) 1263–1268.
[29] F. Haque, D.J. Lloyd, D.T. Smallwood, C.L. Dent, C.M. Shanahan, A.M. Fry, R.C. Trembath, S. Shackleton, SUN1 interacts with nuclear lamin A and cytoplasmic nesprins to provide a physical connection between the nuclear lamina and the cytoskeleton, Mol. Cell. Biol. 26 (2006) 3738–3751.
[30] D.M. Hodzic, D.B. Yeater, L. Bengtsson, H. Otto, P.D. Stahl, Sun2 is a novel mammalian inner nuclear membrane protein, J. Biol. Chem. 279 (2004) 25805–25812.
[31] G. Rabut, V. Doye, J. Ellenberg, Mapping the dynamic organization of the nuclear pore complex inside single living cells, Nat. Cell Biol. 6 (2004) 1114–1121.
[32] J. Gotzmann, S. Vlcek, R. Foisner, Caspase-mediated cleavage of the chromosome-binding domain of lamina-associated polypeptide 2 alpha, J. Cell Sci. 113 (2000) 3769–3780.
[33] Y.Y. Zhen, T. Libotte, M. Munck, A.A. Noegel, E. Korenbaum, NUANCE, a giant protein connecting the nucleus and actin cytoskeleton, J. Cell Sci. 115 (2002) 3207–3222.
[34] A.A. Noegel, R. Blau-Wasser, H. Sultana, R. Muller, L. Israel, M. Schleicher, H. Patel, C.J. Weijer, The cyclase-associated protein CAP as regulator of cell polarity and cAMP signaling in *Dictyostelium*, Mol. Biol. Cell 15 (2004) 934–945.
[35] T. Dechat, J. Gotzmann, A. Stockinger, C.A. Harris, M.A. Talle, J.J. Siekierka, R. Foisner, Detergent-salt resistance of LAP2alpha in interphase nuclei and phosphorylation-dependent association with chromosomes early in nuclear assembly implies functions in nuclear structure dynamics, EMBO J. 17 (1998) 4887–4902.
[36] A. Persson, S. Hober, M. Uhlen, A human protein atlas based on antibody proteomics, Curr. Opin. Mol. Ther. 8 (2006) 185–190.
[37] C. Dreuillet, J. Tillit, M. Kress, M. Ernoult-Lange, In vivo and in vitro interaction between human transcription factor MOK2 and nuclear lamin A/C, Nucleic Acids Res. 30 (2002) 4634–4642.
[38] S.A. Adam, R.S. Marr, L. Gerace, Nuclear protein import in permeabilized mammalian cells requires soluble cytoplasmic factors, J. Cell Biol. 111 (1990) 807–816.
[39] C. Favreau, R. Bastos, J. Cartaud, J.C. Courvalin, P. Mustonen, Biochemical characterization of nuclear pore complex protein gp210 oligomers, Eur. J. Biochem. 268 (2001) 3883–3889.
[40] R.D. Moir, M. Yoon, S. Khuon, R.D. Goldman, Nuclear lamins A and B1: different pathways of assembly during nuclear envelope formation in living cells, J. Cell Biol. 151 (2000) 1155–1168.
[41] J.L. Broers, B.M. Machiels, G.J. van Eys, H.J. Kuijpers, E.M. Manders, R. van Driel, F.C. Ramaekers, Dynamics of the nuclear lamina as monitored by GFP-tagged A type lamins, J. Cell Sci. 112 (1999) 3463–3475.
[42] T. Shimi, T. Koujin, M. Segura-Totten, K.L. Wilson, T. Haraguchi, Y.J. Hiraoka, Dynamic interaction between BAF and emerin revealed by FRAP, FLIP, and FRET analyses in living HeLa cells, Struct. Biol. 147 (2004) 31–41.
[43] Y. Okada, T. Suzuki, Y. Sunden, Y. Orba, S. Kose, N. Imamoto, H. Takahashi, S. Tanaka, W.W. Hall, K. Nagashima, H. Sawa, Dissociation of heterochromatin protein 1 from lamin B receptor induced by human polyomavirus agnoprotein: role in nuclear egress of viral particles, EMBO Rep. 6 (2005) 452–457.
[44] M. Bucci, S.R. Wente, In vivo dynamics of nuclear pore complexes in yeast, J. Cell Biol. 136 (1997) 1185–1199.
[45] C.J. Malone, W.D. Fixsen, H.R. Horvitz, M. Han, UNC-84 localizes to the nuclear envelope and is required for nuclear migration and anchoring during *C. elegans* development, Development 126 (1999) 3171–3181.
[46] J.F. Collet, J.C. Bardwell, Oxidative protein folding in bacteria, Mol. Microbiol. 44 (2002) 1–8.
[47] A.R. Frand, J.W. Cuozzo, C.A. Kaiser, Pathways for protein disulphide bond formation, Trends Cell Biol. 10 (2000) 203–210.
[48] J.M. Mislow, J.M. Holaska, M.S. Kim, K.K. Lee, M. Segura-Totten, K.L. Wilson, E.M. McNally, Nesprin-1alpha self-associates and binds directly to emerin and lamin A in vitro, FEBS Lett. 525 (2002) 135–140.
[49] S. Kandert, Y. Luke, T. Kleinhenz, S. Neumann, W. Lu, V.M. Jaeger, M. Munck, M. Wehnert, C.R. Muller, Z. Zhou, A.A. Noegel, M.C. Dabauvalle, I. Karakesisoglou, Nesprin-2 giant safeguards nuclear envelope architecture in LMNA S143F progeria cells, Hum. Mol. Genet. 16 (2007) 2944–2959.
[50] Y. Lüke, H. Zaim, I. Karakesisoglou, V.M. Jaeger, L. Sellin, W. Lu, M. Schneider, S. Neumann, A. Beijer, M. Munck, V.C. Padmakumar, J. Gloy, G. Walz, A.A. Noegel, Nesprin-2 Giant (NUANCE) maintains nuclear envelope architecture and composition in skin, J. Cell Sci. 121 (2008) 1887–1898.
[51] M. Ketema, K. Wilhelmsen, I. Kuikman, H. Janssen, D. Hodzic, A. Sonnenberg, Requirements for the localization of nesprin-3 at the nuclear envelope and its interaction with plectin, J. Cell Sci. 120 (2007) 3384–3394.
[52] P.J. Stewart-Hutchinson, C.M. Hale, D. Wirtz, D. Hodzic, Structural requirements for the assembly of LINC complexes and their function in cellular mechanical stiffness, Exp. Cell Res. 314 (2008) 1892–1905.